New insights into the chemical composition of five Oort Cloud comets after re-analysis of their infrared spectra

Manuela Lippi[1,2], Geronimo L. Villanueva[1], Michael J. Mumma[1], Maria N. Camarca[1,2], Sara Faggi[1,2], Lucas Paganini[1,3]

[1] NASA Goddard Space Flight Center, 8800 Greenbelt Rd., Greenbelt, MD, 20771, USA

[2] American University, Dept. of Physics, 4400 Massachusetts Ave NW, Washington, DC 20016, USA

[3] NASA Headquarters, 4th street, Washington, DC 20546

Abstract

We present revised results for the main molecular species in five Oort Cloud (OC) comets observed with NIRSPEC at the Keck Observatory between 1999 and 2012 (C/1999 S4 (LINEAR), C/2001 A2 (LINEAR), C/2007 W1 (Boattini), C/2012 F6 (Lemmon), and C/2012 S1 (ISON)). The re-evaluation of these data shows the improvement of results in some of the datasets, in particular for comets observed and analyzed before the advent of new and revised fluorescence models and terrestrial retrieval methods introduced since 2011. We observe significant improvements in the resulting rotational temperatures and production rates for all species, and in mixing ratios of minor species (relative to water). The re-analysis also allowed us to quantify species not analyzed previously, mostly due to the lack of molecular models (e.g., ammonia and formaldehyde). We note, however, that the improvement of these revised values is less substantial for comets observed (and/or analyzed) since 2010.

Keywords: *comets – spectroscopy, composition, taxonomy; astrobiology*

Corresponding author: Manuela Lippi – mlippi@american.edu, manuela.lippi@nasa.gov

1. Introduction

Cometary nuclei are cryogenically preserved relics from the early Solar System. Their compositional properties (molecular abundances, isotopic ratios, spin temperatures) are directly relevant to understanding the processes affecting material during Solar System formation; moreover, they could test the hypothesis that small icy bodies have delivered prebiotic matter to early Earth. Current theories suggest that cometary nuclei probably formed from the ice and dust present in the protoplanetary disk at distances between 5 and 30 AU from the proto-sun; after their formation, they were ejected to their current reservoirs – the Kuiper Belt and the Oort cloud – as a result of gravitational interactions with the migrating giant planets (Gomes 2005, Morbidelli et al. 2007). Even if diverse processes (such as energetic radiation and collisions) partially altered the chemical fingerprints of nucleus surface layers during their lifetime prior to injection into the inner solar system, the bulk nucleus is thought to preserve certain local chemical and mineralogical properties related to the protoplanetary disk where they formed. Our study seeks an accurate chemical classification of comets, to unveil important information regarding the origins and evolution of the early Solar System and to understand the true heritage of these icy bodies.

A powerful technique to sample the organic composition of comets is the use of high-resolution spectroscopy in the infrared region between about 3 and 5 μm, where it is possible to sample emission lines produced by solar-pumped fluorescence of molecules released directly from the nucleus, such as H_2O, CH_4, C_2H_6, C_2H_2, HCN, NH_3, CH_3OH, H_2CO, and CO. With this technique, we can investigate cosmogonic indicators like molecular abundances, isotopic ratios, ortho-para ratios and spin temperatures that are expected to remain unaltered since the comet's formation. Since 1996, high-resolution ($\lambda/\Delta\lambda \geq 25{,}000$) spectra of comets in the infrared region were acquired using ground-based echelle spectrometers. We have created a database collecting all spectra obtained from more than 60 comets using state-of-the-art high-resolution IR spectrometers (e.g., IRTF/CSHELL, Keck/NIRSPEC and VLT/CRIRES). The correct modeling and analysis of these data is essential to interpreting important clues regarding the aforementioned cosmogonic indicators in comets, and to constraining the conditions present where (and when) a specific comet formed.

Recent taxonomic reviews (cf., Mumma & Charnley 2011, Dello Russo et al. 2016, Bockelée-Morvan & Biver 2017) are based on primary volatiles in about 30 comets and have revealed a wide compositional diversity, but it is clear that an understanding of these bodies is far from complete. Some infrared results published before 2010 may contain systematic inaccuracies introduced by the use of immature algorithms and/or incomplete molecular models used to interpret the fluorescence excitation in comets.

In particular, fluorescence models for some individual ro-vibrational bands have evolved with time, affecting the production rates derived from measured line fluxes. In the past, certain molecular models made use of empirical line strengths when calculating the fluorescence efficiencies (g-factors) to interpret the IR fluorescence excitation in comets. While these models were in part accurate, they were sometimes limited to only a few spectral lines and also did not fully describe the complexity of some observed spectra, often under-estimating or ignoring fluorescence cascades. The discovery of H_2O hot-band emissions in 1P/Halley with the Kuiper Airborne Observatory (KAO) revealed their importance (Weaver et al. 1986), and an early model of H_2O fluorescence spectra included several hot-bands (e.g., Bockelée-Morvan & Crovisier 1989). The (later) need to identify a method for direct detection of cometary water from ground-based observatories led to the use of hot-band emission as a way to circumvent telluric extinction (Mumma et al. 1995); its first general application used the 2 μm hot-bands to characterize water in comet C/1996 B2 Hyakutake (Mumma et al. 1996). This initial success, and the team's serendipitous detection of H_2O hot-band emission near 4.7 μm in Hyakutake, led to the extended use of water hot-bands in C/1995 O1 (Hale-Bopp) and later comets (Dello Russo et al. 2005). Searches for trace gases (HCN, H_2CO, CH_3OH, CH_4, C_2H_2, C_2H_6) emphasized their fundamental bands (e.g., HCN, Magee-Sauer et al. 2002; H_2CO, DiSanti et al. 2006; and CH_4, Gibb et al. 2003), leading to successful detections and increasingly robust interpretations. But, they too underwent successive improvements and updates as new band analyses emerged.

Since 2011, realistic quantum band models have been developed for many species, including complete line lists for specific vibrational bands, updated energy tables, and corrections for the Swings effect (i.e., the dependence on heliocentric velocity; e.g., Villanueva et al. 2011b, Villanueva et al. 2012b). Figure 1 shows an example of the remarkable differences between cometary fluorescence models before and after 2011. By providing more precise g-factors and including weak

lines that were not considered in some of the previous analyses, these models now allow investigation of the spectra with unprecedented accuracy, thus enabling retrieval of more precise rotational temperatures. An improvement between predicted and observed line fluxes translates to a lower relative error for the rotational temperature (and consequently, for the temperature-dependent g-factors) and retrieved production rates. The development of quantum band models for many molecular species, revealed also the remarkable complexity present in many spectral regions. This has increased the ability to recognize blended lines, which otherwise would lead to inaccurate production rates and mixing ratios – especially important for spectrally dense regions such as the CH-stretch near 3.32-3.54 μm. Furthermore, some molecules were not investigated in some comets analyzed before 2002, owing to the lack of specific molecular models (e.g., NH_3 or H_2CO), for instance, in comets C/1999 S4 (LINEAR) and C/2001 A2 (LINEAR); here, we provide the first analysis of NH_3 and H_2CO in them.

We recently updated our data reduction procedures used for the analysis of ground-based observations, which have greatly improved the spectral calibration through improved modeling of the Earth's atmospheric transmittance and thus a better assessment of the terrestrial corrections needed for observed cometary spectra. In the past 20 years, different radiative transfer models have been used to synthesize the terrestrial atmospheric transmittance at high spectral resolution: the Spectrum Synthesis Program (SSP) accessing HITRAN 1992 (Kunde and Maguire 1974, Rothman 1992), the General Line-by-Line atmospheric transmittance and radiance model (GENLN, Edwards 1992, and the Line-By-Line Radiative Transfer Model (LBLRTM - Clough et al 2005), models that were further improved with the incorporation of complete and comprehensive databases for water (Villanueva et al. 2012b), ethane (Villanueva et al. 2011b) and carbon dioxide (Villanueva et al. 2008a). We now use the Planetary and Universal Model of Atmospheric Scattering (PUMAS - Villanueva et al. 2018). PUMAS uses realistic profiles from the latest atmospheric database produced by NASA's Modern-Era Retrospective Analysis for Research and Applications (MERRA-2, Gelaro et al. 2018), and the latest radiative-transfer methods and spectroscopic parameters to calculate a line-by-line, layer-by-layer, radiative transfer model for the terrestrial atmosphere under the specific observational conditions.

Considering that data analysis techniques and molecular and atmospheric models have evolved and improved greatly since 1996, a chemical classification of comets may be affected by systematic uncertainties introduced by different reduction and retrieval approaches. This is expected to impact mostly comets that were observed before 2011 – when we introduced the new analysis approaches – which constitute the majority of targets in our database (see Figure 2).

Here, we present updated rotational temperatures and production rates (and mixing ratios relative to water) for five OC comets (C/1999 S4 (LINEAR), C/2001 A2 (LINEAR), C/2007 W1 (Boattini), C/2012 F6 (Lemmon) and C/2012 S1 (ISON), hereafter S4, A2, W1, F6, S1, respectively), using data selected from our rich archival dataset. By the re-analysis of five OC comets, we seek an initial evaluation to quantify these inaccuracies. The comparison of current and earlier results for W1, F6 and S1 confirm the validity of the current reductions, while the current results for S4 and A2 present updated or even entirely new values for them. Thanks to the aforementioned improvements in the data retrieval process, our re-analysis of these spectra demonstrates that we can now unlock new and improved information from these datasets, especially for comets observed and analyzed prior to 2011.

2. Data acquisition and reduction

The data presented in this paper were obtained with the near-infrared echelle grating spectrometer (NIRSPEC) at the W. M. Keck Observatory (McLean et al. 1998), located on Mauna Kea, Hawaii. In Table 1, we summarize the observing logs for the five comets along with a list of sampled molecules. For more details, we refer the reader to the original publications: Mumma et al. 2001 for S4, Magee-Sauer et al. 2008 and Gibb et al. 2007 for A2, Villanueva et al. 2011a for W1, Paganini et al. 2014 for F6 and DiSanti et al. 2016 for S1.

We processed all datasets in a systematic way using semi-automated tools to improve processing speed and minimize possible human errors. These tools include the latest procedures for flat fielding, removal of high dark current pixels and cosmic ray hits, along with spatial and spectral straightening with milli-pixel precision. Spectral calibration and compensation for telluric absorption is achieved by comparing the data with highly precise atmospheric radiance and transmittance models obtained

with PUMAS. Flux calibration was obtained using the archived observations of a suitable standard star (observed closely in time with the comet) and our current data reduction algorithms.

To retrieve rotational temperatures (T_{rot}) and production rates (Q) we performed two different and independent analyses: a χ^2 minimization technique (using a Levenberg-Marquardt fitting algorithm) and a correlation analysis (for more details on these methodologies see Villanueva et al. 2008 and Bonev 2005, respectively). It has been demonstrated that these two methods are highly complementary, and they converge to a unique solution for T_{rot}, validating the robustness of the retrieval approach (see Bonev et al. 2013).

Once T_{rot} is determined, we calculate line production rates (Q_{line}) using the following formula:

$$Q_{line} = GF \frac{4\pi\Delta^2 F_{line}}{\tau_{mol} f(x) g_{line}}$$

where F_{line} is the line flux (W/m^2, corrected for telluric transmittance), Δ is the geocentric distance (AU), τ_{mol} is the molecular photodissociation lifetime of the considered molecule (in seconds and calculated for a heliocentric distance of 1 AU), and $f(x)$ is a function representing the fraction of all molecules in the coma contained in the beam (spherically symmetric uniform outflow is assumed, see appendix in Hoban et al 1991); g_{line} is the line g-factor (W molecule^{-1}) calculated at the correct rotational temperature (and for a heliocentric distance of 1 AU), while GF is a "growth factor", accounting for slit losses and aperture effects, and derived by comparing the column abundance measured at discrete nucleocentric distances with outflow and photolysis models for the molecule in question (for detailed discussions of the "Q-curve" formalism see Villanueva et al. 2011a, Appendix B2 in Bonev et al. 2006, Dello Russo et al. 1998, Mumma et al. 2003). The final production rate for a certain molecular species is computed as the weighted average of total production rates resulting from individual emission lines.

We report rotational temperatures, production rates, and mixing ratios (MR) of (minor) volatile species with respect to water. For detections, the uncertainty in production rate is taken as the larger of the stochastic and standard noise contributions; statistical uncertainties are then propagated quadratically. If lines are not clearly detected for a given molecule, we provide upper limits at 3σ,

calculated as three times the uncertainties retrieved through the covariance matrix of the Levenberg-Marquardt fitting algorithm scaled for the goodness of the fit (i.e. the square root of the reduced χ^2).

3. Results and comparison

3.1. C/1999 S4 (LINEAR)

Comet C/1999 S4 was discovered on 1999, September 27th (IAU Circular 7267), and after several outbursts it was declared extinct in mid-August 2000. The retrieval of rotational temperatures and production rates for this comet was impacted by an unusually large water content in Earth's atmosphere during the observing night, resulting in low transmittance in some spectral regions. Moreover, the comet showed a very bright dust continuum but weak emission lines. Even so, we identify multiple water lines resulting in a rotational temperature of (75 ± 5) K, and we measure different water production rates depending on the used setting. These measurements are consistent with an exponential decrease in water production rate over time (see Figure 3), possibly related to the peculiar outgassing behavior of comet S4, which was characterized by significant increase/decrease of its activity before disruption (e.g., a minor outburst on July 13th; Bockelée-Morvan et al. 2001, Farnham et al. 2001, and references therein). Unfortunately, we were not able to verify that other molecules exhibited a similar behavior.

In addition to water, we detect C_2H_6, CH_4, HCN and CO, and retrieve (3σ) upper limits for NH_3, C_2H_2, H_2CO and CH_3OH. Since water showed a strong variation during the night, our mixing ratios are calculated using the individual H_2O production rates, depending on the considered setting. Production rates and mixing ratios (with respect to water) are summarized in Table 2; and an example of extracted spectra for comet S4 is shown in Figure 4 – panel A.

Our results differ in many ways from those presented in Mumma et al. 2001 (see Figure 5 and Tables 3 - 5), owing largely to the maturation of molecular fluorescence models and of data reduction algorithms**.** The new quantum molecular models and the updated atmospheric models play important roles in the updated results for this comet. The ability to sample multiple lines of water yielded a higher rotational temperature (+50%), and distinct production rates for the three settings used. Previously, Mumma et al. 2001 identified and used two water lines in MW setting and assumed

a fixed T_{rot} of 50 K, based on observations of only 8 comets before S4. They did not reduce water lines from the KL1 and KL2 settings since suitable fluorescence models were not available then. If we use their rotational temperature to retrieve water from the KL1 spectra, the production rate that we obtain is ((650 ± 50) x 10^{26} mol/s), lower than the weighted mean from OH* (prompt emission) in the KL1 and KL2 settings presented in Mumma et al. 2001 ((730 ± 50) x 10^{26} mol/s)).

Dello Russo et al. (2005) re-analyzed the S4 spectra using a then-updated water fluorescence model, retrieving a corresponding rotational temperature of 73^{+8}_{-6} K and a water production rate of (677 ± 51) x 10^{26} mol/s (see Tables 3 and 4). To our knowledge, values for trace gases were not re-analyzed with the updated temperature, excepting methane (for an assumed rotational temperature of 70 K, Gibb et al. 2003 reported a production rate of (1.0 ± 0.3) x 10^{26} mol/s and a mixing ratio of (0.18 ± 0.06)%). The current analysis is the first to update values for all trace gases using self-consistent and modern algorithms and procedures.

In the 3310 cm^{-1} spectral region, our analysis of C_2H_2 and HCN gives production rates that are substantially lower than those in previous publications. This spectral region contains several spectral lines from different molecular species, whose overlap, if not accounted for, can lead to erroneous production rates. Moreover, before 2001 several specific molecular models did not exist (e.g., NH_3) or were deficient (e.g., H_2O), resulting in an incomplete picture of the spectra. For example, the water line at about 3320 cm^{-1} was not modeled in the previous analysis of S4, so its potential blend with a spectral line of HCN (R2) resulted in a higher production rate for HCN. Later studies omitted the R2 line from HCN analyses for this reason (for example, the study of 2001 A2 by Magee-Sauer et al. 2008, see below). With the mature post-2011 algorithms, we can include it since we solve for all molecules simultaneously using the Levenberg-Marquardt formalism. The HCN production rate retrieved including the updated water molecular model and using a rotational temperature of 50 K results in (0.10 ± 0.04) x 10^{26} mol/s, a lower value than the previous result of (0.61 ± 0.17) x 10^{26} mol/s.

Finally, we report the first upper limits for NH_3 and H_2CO; their fluorescence models were lacking in 2001 and thus their production rates were not reported in previous work.

3.2. C/2001 A2 (LINEAR)

Comet A2 was discovered on 2001, January 15th (IAU Circular 7564); this comet was characterized by several outbursts and breakups, offering the possibility to study fresh organic material released from the nucleus. Observations and data reduction were complicated by poor weather conditions and by a reduced sensitivity of the spectrometer, especially in the region near 3.0 μm, due to the presence of water ice on a mirror within the instrument. Nevertheless, A2 showed many bright molecular emission lines, allowing us to retrieve individual rotational temperatures for H_2O, C_2H_6, CH_3OH, and HCN (Table 6). The rotational temperatures for H_2O, C_2H_6, and CH_3OH are consistent with the weighted mean of (85 ± 5) K, and adopting this value for all molecular species results in the production rates and corresponding mixing ratios shown in Table 7; Figure 4 – panel B shows the detection of CH_3OH on 2001, July 9th.

Our reanalysis of data from comet A2 presents important new insights into its chemical composition. Like comet S4, the new quantum molecular models and the updated atmospheric transmittance play important roles in our analysis. Our retrieved rotational temperatures for H_2O, C_2H_6, and HCN are slightly smaller and less dispersed than those of Magee-Sauer et al. 2008 (see Table 6), and they agree with our newly retrieved T_{rot} for CH_3OH. Our rotational temperature for HCN is significantly lower than that for H_2O (and other trace species), in agreement with previous findings. The lower temperature for HCN suggests that it arose farther from the nucleus than the native species, perhaps owing to extended release; our measured growth factors for HCN and H_2O are similar, and this is consistent if release is centered along the line of sight. Further discussion will be given elsewhere.

Our production rates for H_2O are smaller than those of Magee-Sauer et al. 2008 (about 30% lower, see Table 8). Using the modern algorithms, the current mixing ratios are smaller for HCN, H_2CO, CO and C_2H_2, but greater for CH_3OH, C_2H_6 and CH_4 (see Table 9 and Figure 6). The lower production rate for water is noticeable even when we run our models with the rotational temperatures used in previous publications. For example, if we use the rotational temperature of 105K reported by Magee-Sauer et al. 2008 for observations of UT 10.5 July 2001, we obtain a water production rate of (343 ± 26) x 10^{26} mol/s. This is about 20% lower than the previously reported value of (430 ± 37) x 10^{26} mol/s (Magee-Sauer et al. 2008).

Our rotational temperature and production rates for CH_3OH are consistent with recent results in Villanueva et al. 2012a, that used the same molecular fluorescence model (i.e., g-factors); however, they adopted water production rates from Magee-Sauer et al. 2008, so their reported mixing ratio differs from our value. Finally, we report a 3σ upper limit for NH_3 mixing ratio, not investigated before.

3.3. C/2007 W1 (Boattini)

Comet W1 is a dynamically new comet discovered in 2007 (IAU Circular 8899). The observing conditions for this comet were highly favorable during its passage through the inner Solar System, with perihelion at 0.85 AU and closest approach to the Earth at 0.21 AU, making this an optimal target for spectroscopic observations.

We retrieve rotational temperatures for H_2O, C_2H_6, CH_3OH and HCN, and using an averaged value of (83 ± 3) K we report revised production rates and mixing ratios for H_2O, C_2H_6, CH_3OH, HCN, C_2H_2, NH_3, CH_4, and CO, and an upper limit (3σ) for H_2CO (see results in Table 10 and a spectrum from W1 in Figure 4 – panel C). In our analysis we scaled the nucleus-centered production rates with the retrieved growth factors; we then applied an additional correction factor of 2.5 to production rates of water and methanol (see footnote 'd' in Table 3 of Villanueva et al. 2011a) .

Given that Villanueva et al. 2011a used some of the latest reduction techniques and fluorescence models, we note minor differences in the two results (see Figure 7 and Tables 11, 12 and 13). We obtain similar rotational temperatures for all the molecular species, and a lower production rate for water (about -10%); the trace species show mixing ratios that are consistent (within ± 1σ confidence limits) with the previous results, except for CH_3OH (about +11%) and C_2H_6 (about +18%).

The observed differences in mixing ratios are mainly related to our lower value for the water production rate. For example, Villanueva et al. 2011a reported the modeling of only the Q-branch of CH_3OH ν_3 band – as opposed to the full ro-vibrational band model that we apply for the current analysis; moreover, they don't include Q-scale uncertainties propagation in the calculation of the mixing ratios.

If we follow a similar approach, limiting our analysis to the Q-branch observed on UT 9 July 2008 and before applying the 2.5 correction factor, we obtain a methanol production rate of (4.49 ± 0.34)

x 10^{26} mol/s — comparable with the value of ((4.42 ± 0.34) x 10^{26} mol/s) previously reported and only about 4% smaller than the value we retrieve by considering the complete ν_3 band ((4.67 ± 0.36) x 10^{26} mol/s). If we use our Q-branch value along with the previously published water production rate, we retrieve a methanol mixing ratio of (3.73 ± 0.12)%, which is similar to the one published in Villanueva et al. 2011a (3.67 ± 0.11)%.

3.4. C/2012 F6 (Lemmon)

Comet F6 was discovered on 23rd March 2012 and belongs to the nearly isotropic long period comet group, originating from the Oort Cloud. For observations on 20th June 2012, we retrieve a water rotational temperature of (53 ± 3) K, production rates for H_2O, C_2H_6, CH_3OH, HCN and NH_3, and 3σ upper limits for C_2H_2 and H_2CO. Observations of methane were precluded by the low geocentric velocity of the comet and CO was not sampled. The results are summarized in Table 14 and a sample extracted spectrum is shown in Figure 4 – panel D. These data were originally presented in Paganini et al. 2014, which used similar procedures and molecular models. Thus, as expected, our values are consistent within 1σ confidence limits (see Figure 8 and Tables 15, 16 and 17), excepting formaldehyde for which we found a smaller upper limit. This difference is probably related to the fact that for non-detections our 3σ upper limits are calculated using the uncertainties retrieved through the covariance matrix of the Levenberg-Marquardt fitting algorithm, while previous reductions consider the uncertainties retrieved from the correlation analysis.

3.5. C/2012 S1 (ISON)

Discovered on 2012 September 21st, C/2012 S1 (known as D/2012 S1 after its disruption) was a dynamically new sun-grazing comet that disintegrated as it passed close to the Sun; NIRSPEC observing runs are listed in Table 1. Except on the night of November 7th, the comet did not show very bright lines and the spectra were quite noisy, limiting the possible molecular detections. In Figure 4 – panel E we show the detection of water on November 7th. We report our results in Table 18.

Even though comet S1 was observed and analyzed quite recently, we find some differences between our results and those presented in DiSanti et al. 2016 (see Figure 9 and Tables 19, 20 and

21). We obtained robust water rotational temperatures for October 25th and November 7th, showing a slight increase of temperature in November, and our production rates for water are consistent with those of DiSanti et al. 2016. Our mixing ratios for HCN, C_2H_6 and CH_4 are higher, while we get the same value for C_2H_2. Due to the low signal-to-noise ratio, we report only upper limits for CH_3OH and H_2CO, that are consistent with values reported previously, as well as upper limits for CO and NH_3. Despite these differences, our results are in agreement within 1σ confidence limits with DiSanti et al. 2016.

4. Discussion

In the previous section we showed that for comets S4 and A2, observed and analyzed before 2011, the results obtained with the updated models and procedures differ significantly from previous work. For comets W1, F6 and S1, we notice some differences with respect to previous rotational temperatures, production rates, and mixing ratios, but the results are in general consistent within confidence limits. We find that these discrepancies are likely due to the inherent uncertainties related to the noise of the astronomical observations and (slight) human interaction in the data analysis. However, we observe improvements to pre-2011 work, and we attribute these changes to the following factors:

- New and improved quantum fluorescence molecular models. Using the new models, the rotational temperatures, production rates, and mixing ratios are better constrained thanks to more precise g-factors, more complete molecular line lists, and availability of improved molecular constants. These breakthroughs have facilitated the analysis of spectral regions characterized by overlapping of emission lines from different molecules (e.g., the HCN spectral region). Furthermore, the development of new models has allowed the characterization of species not reported in previous studies.
- Implementation of updated atmospheric models. An accurate model of the terrestrial transmittance at the times of observation is necessary to assist in the reduction and calibration of spectroscopic data collected using ground-based observations. Inaccuracies in the atmospheric models translate into an improper removal of terrestrial features, which affects the characterization

of the comet's continuum and can critically affect the modeled atmospheric transmittance at the Doppler-shifted position of an individual line.

- Novel approaches for the retrieval of the molecular properties. The χ^2 minimization technique and the correlation analysis are two different and independent methods that can be used for the analysis of the spectral features. When used together, their convergence to a common solution for rotational temperatures and production rates is a test that can verify the self-consistency of the results. The χ^2 minimization technique could not be used before the advent of advanced quantum molecular models.
- A systematic study of the flux calibration. Flux calibration is one of the key steps in reducing spectra: for this reason, we have recalculated the flux calibration factors for each observation, using the semi-automatic procedure and the updated atmospheric transmittance models; we then compared all the calibration factors from different observing campaigns, cross-checking for their consistency.

The significant differences observed in pre-2011 results could bring strong implications to our understanding of cometary taxonomy, and the addition of new molecular species (e.g., NH_3 and H_2CO) in the infrared database can further our understanding of cometary origins. For example, in Figure 10, we show how the relationship between HCN and C_2H_6 mixing ratios investigated in previous reviews (e.g. Mumma & Charnley, 2011, Dello Russo et al., 2016) changes if we consider the results presented in our new analysis. Since the mixing ratios retrieved from about 58% of comets present in our database need revision (see Figure 2), we expect that the updated results will impact on molecule-to-molecule relationships, with the greater impact for those species that are at the moment poorly determined (e.g., NH_3 and H_2CO). But, to infer more definite conclusions we will first need to complete our revisions, as exemplified by the sample results presented here.

4.1. Comparison and classification of comets

We can make use of the updated results to retrieve some information about the possible origins of the analyzed comets. When comparing abundances of trace species, two comets can share the same relative amount of the individual molecules, although absolute values of mixing ratios can appear very different. For this reason, we decided to consider pie charts to show how the elements are proportionally distributed in a given comet (see Figure 11). In theory these proportions are related to the processes that affected a comet during its formation and its history and can give valuable clues on cometary taxonomy. For the trace species we created multilevel pies, where the inner level takes into consideration a possible chemical formative origin, resulting in the following four representative sub-groups:

- Group 1 – CO (red): it is one of the most hyper-volatile species in cometary coma and most likely has interstellar origin
- Group 2 – CH_3OH, H_2CO and CH_4 (yellow): methanol and formaldehyde may form through hydrogenation of condensed CO, while hydrogenation of atomic C trapped in CO ice can produce methane (Hiraoka et al. 1994, Hiraoka et al. 1998).
- Group 3 – C_2H_2 and C_2H_6 (blue): hydrogenation of acetylene can produce ethane (Hiraoka et al. 2000).
- Group 4 – HCN (green).

The outer band of each pie shows the proportional amount of individual molecular species using corresponding color shades; the proportion between water and all other species considered here is also reported in an additional pie. The NH_3 molecule was not included because for comets S4, A2 and S1 it is not detected with NIRSPEC, and the corresponding retrieved upper limits are not significant if compared with the NH_3 average found in other Oort Cloud comets, leading to possible bias in the pies.

If we organize the multilevel pies with decreasing CO, we can see a gradient in their redox ratio (sum of H_2CO, CH_3OH, and CH_4 relative to CO) that ranges from 0.37 (S4) to 2.25 (W1): the five comets are quite distinct in redox ratio, excepting F6 and S1 with redox ratios of 0.58 and 0.61 respectively.

Considering the second group (CH_3OH, H_2CO and CH_4), comet F6 is more similar to S1 and S4, even though the proportion of methanol in the latter is lower; for A2 and W1 the contribution of this group to the total composition is much higher than the other comets.

In the third group (C_2H_2 and C_2H_6), we see that comets S4, S1 and F6 again look similar, showing lower abundance fractions for C_2H_6, opposite to W1 and A2 that show much higher contributions for this molecule – especially in comet A2. Finally, HCN looks quite the same for all compared comets excepting S4 which displays a lower value.

Effective hydrogenation of simple compounds (e.g., CO, C_2H_2) is favored in relatively cold formation environments, where atomic hydrogen is better retained on grain surfaces, and this affects the hydrogenation ratios in pre-cometary ices (Mumma et al. 1996, 2001). If we assume that mixing ratios are cosmogonic indicators of chemical conditions in a given comet's birth-place, the higher redox ratio for C_2H_x in A2 and W1 suggests that they formed in a colder region of the disk than that where S4, S1 and F6 formed. In this colder region, the retention and hydrogenation of CO on pre-cometary grain should also have been more efficient, and indeed the COH_x redox ratio is higher for A2 and W1 compared with S4, S1 and F6. The intermediate hydrogenation product (C_2H_4) has not been detected in any comet, consistent with much faster hydrogenation rates for adsorbed C_2H_4 than for C_2H_2 (cf., Hiraoka et al. 2000). A2 shows a higher proportion of C_2H_6 and a lower one for CH_3OH, consistent with a different hydrogenation history or a different endowment of initial C_2H_2 vs CO with respect to W1. The gradual decrease of the proportion of CO in the compared comets may also suggest a gradient in temperature in the protoplanetary disk.

5. Conclusions and Future Steps

We presented updated production rates, mixing ratios of minor species (relative to water), and rotational temperatures for five comets observed with NIRSPEC at the Keck Observatory since 1999, obtained using more complete fluorescence quantum-band models and stand-alone analysis

techniques. Our results for these comets allowed us to identify certain drawbacks in previous analyses that could limit a true understanding of cometary taxonomy. In particular, we showed that it is possible to obtain significant improvements in datasets that were analyzed before the advent of recent fluorescence models and terrestrial retrieval methods (i.e. before 2011). For instance, we quantified results for ammonia and formaldehyde in comets S4 and A2.

We are now revisiting the 60+ comets in our database to build an updated chemical classification of comets. In addition to the updated mixing ratios, our chemical classification would include comparisons with other cosmic indicators, such as isotopic ratios, ortho-to-para ratios, and spin temperatures. Ultimately, a self-consistent, revised chemical taxonomy would allow the removal of inconsistencies added by dissimilar retrieval strategies and inaccurate (or absent) information due to missing fluorescence efficiencies. As already mentioned, a better understanding of cometary compositions and their possible groupings can help us understand the conditions that shaped our planetary system during its formation, and with this work we demonstrated the need to revisit existing (pre-2011) cometary data. We expect that a re-assessment of certain datasets could provide a more accurate picture of the chemical taxonomy of comets.

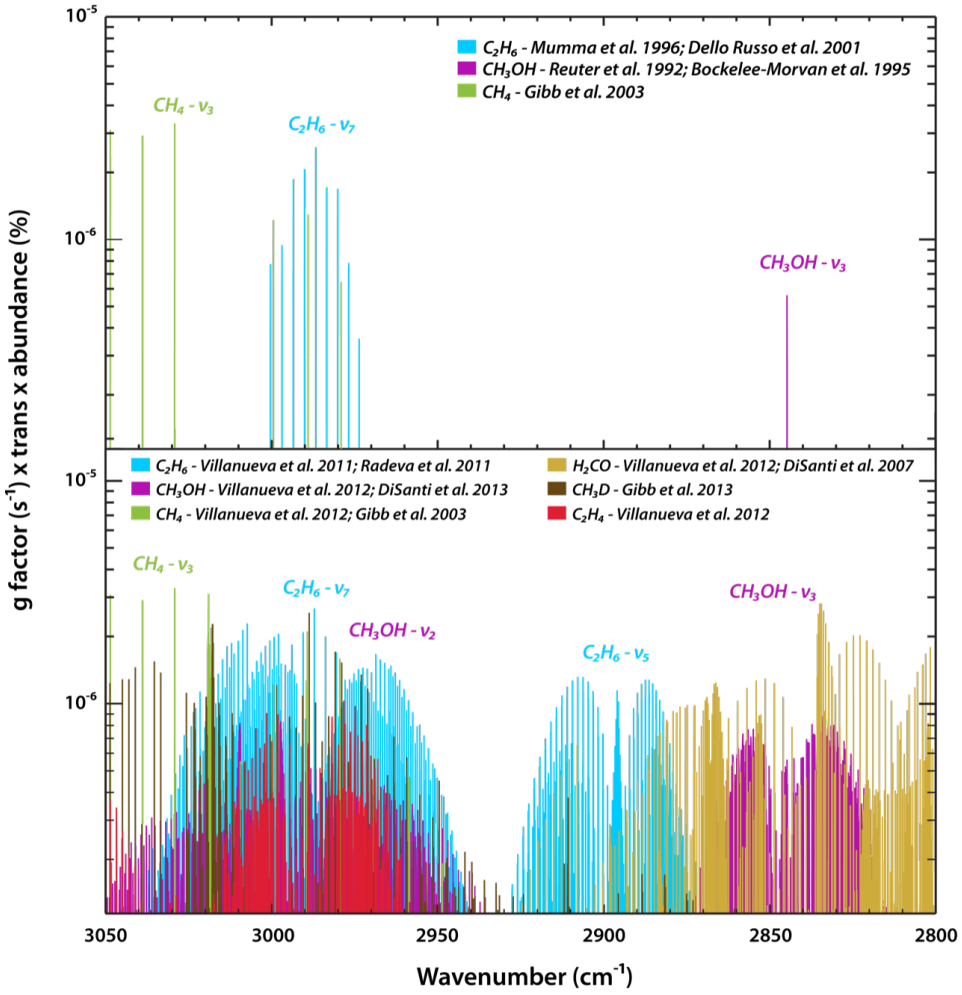

Figure 1. *Example of evolution of molecular models used to interpret fluorescence in comets before (upper panel) and after (lower panel) 2011. The x-axis corresponds to the spectral region between 3050 and 2800 cm^{-1}, while the y-axis corresponds to molecular line fluorescence efficiencies scaled by typical molecular abundances and terrestrial transmittance (for Mauna Kea, HI). In the upper panel empirical g-factors corresponding to the CH_3OH-ν_3 (purple), C_2H_6-ν_7 (cyan), and CH_4-ν_3 (green) ro-vibrational transitions are shown. The same colors are used to represent full quantum molecular models for the same molecules considering also the CH_3OH-ν_2 and C_2H_6-ν_5 ro-vibrational transitions; in the same panel H_2CO (sand), CH_3D (brown) and C_2H_4 (red) quantum molecular models are also shown. References to the different models are reported in the bibliography.*

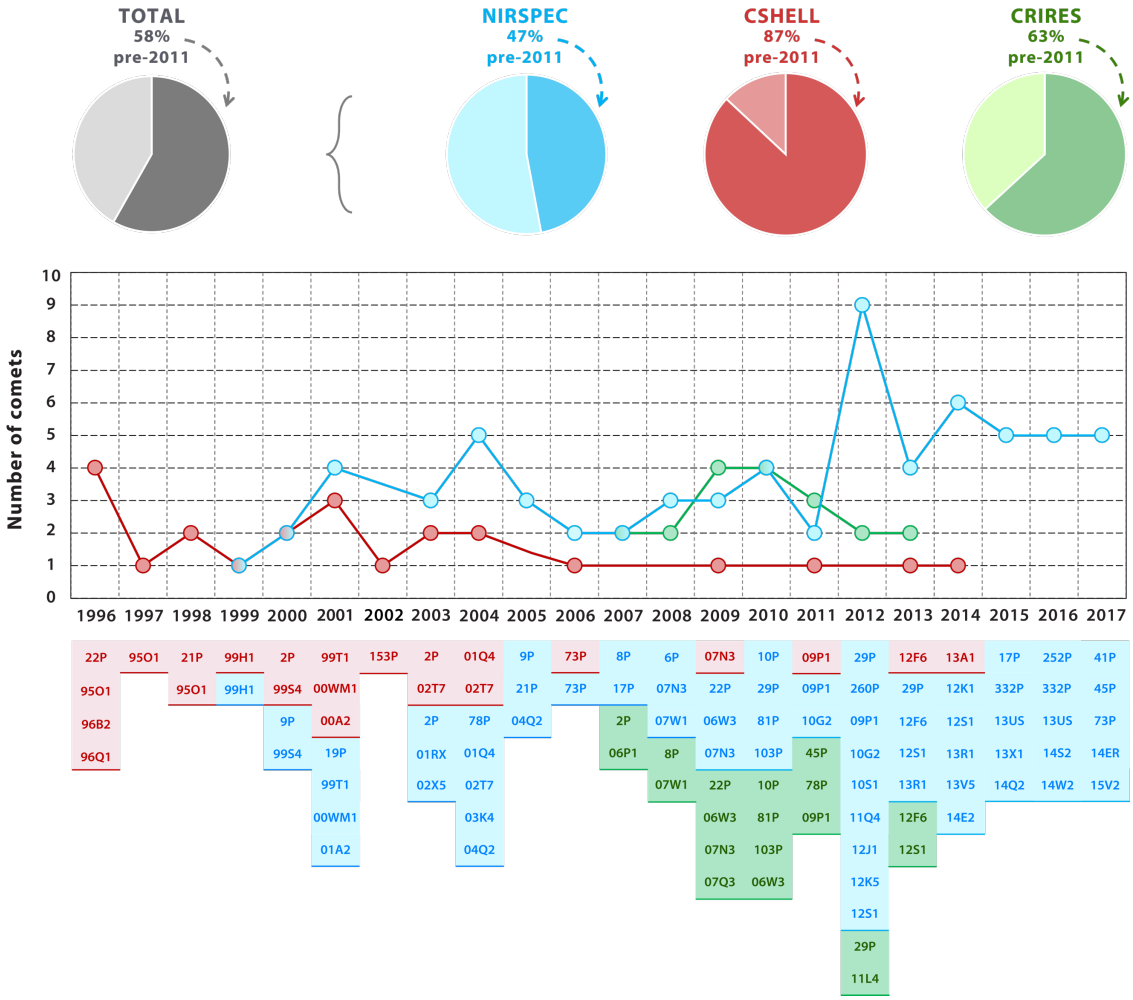

Figure 2. *Observations through time of comets with selected infrared spectrometers (CSHELL in red, NIRSPEC in cyan, CRIRES in green). The pies in the upper part of the figure represent the percent of comets observed before (darker color) and after (lighter color) 2011, for each instrument and considering the total (grey pie). The lower graphic shows the number of comets observed for each year, from 1996 till 2017*[1].

[1] *The acronyms and full comet names are:* ***22P****: 22P/Kopff,* ***95O1****: C/1995 O1 Hale Bopp,* ***96B2****: C/1996 B2 Hyakutake,* ***96Q1****: C/1996 Q1 Tabur,* ***21P****: 21P/Giacobini-Zinner,* ***99H1****: C/1999 H1 Lee,* ***2P****: 2P/Encke,* ***99S4****: C/1999 S4 LINEAR,* ***9P****: 9P/Tempel 1,* ***99T1****: C/1999 T1 McNaught,* ***00WM1****: C/2000 WM1 LINEAR,* ***01A2****: C/2001 A2 LINEAR,* ***19P****: 19P/Borrelly,* ***153P****: 153P/Ikeya-Zhang,* ***02T7****: C/2002 T7 LINEAR,* ***01RX****: C/2001 RX 14 LINEAR,* ***02X5****: C/2002 X5 Kudo-Fujikawa,* ***78P****: 78P/Gehrels 2,* ***01Q4****: C/2001 Q4 Neat,* ***03K4****: C/2003 K4 LINEAR,* ***04Q2****: C/2004 Q2 Machholz,* ***73P****: 73P/Schwassmann–Wachmann (B-C),* ***8P****: 8P/Tuttle,* ***17P****: 17P/Holmes,* ***06P1****: C/2006 P1 McNaught,* ***6P****: 6P/d'Arrest,* ***07N3****: C/2007 N3 Lulin,* ***07W1****: C/2007 W1 Boattini,* ***06W3****: C/2006 W3 Christensen,* ***07Q3****: C/2007 Q3 Siding Spring,* ***10P****: 10P/Tempel 2,* ***29P****: 29P/Schwassmann–Wachmann 1,* ***81P****: 81P/Wild 2,* ***103P****: 103P/Hartley 2,* ***09P1****: C/2009 P1 Garradd,* ***10G2****: C/2010 G2 Hill,* ***45P****: 45/P Honda–Mrkos–Pajdušáková,* ***260P****: 260P/McNaught,* ***10S1****: C/2010 S1 LINEAR,* ***11Q4****: C/2011 Q4 Swan,* ***12J1****: C/2012 J1 Catalina,* ***12K5****: C/2012 K5 LINEAR,* ***12S1****: C/2012 S1 ISON,* ***11L4****: C/2011 L4 Pan-STARRS,* ***12F6****: C/2012 F6 Lemmon,* ***13R1****: C/2013 R1 Lovejoy,* ***13A1****: C/2013 A1 Siding Spring,* ***12K1****: C/2012 K1 Pan-STARRS,* ***13V5****: C/2013 V5 Oukaimeden,* ***14E2****: C/2014 E2 Jacques,* ***332P****: 332P/Ikeya Murakami,* ***13US****: C/2013 US10 Catalina,* ***13X1****: C/2013 X1 Pan-STARRS,* ***14Q2****: C/2014 Q2 Lovejoy,* ***252P****: 252P/LINEAR,* ***14S2****: C/2014 S2 Pan-STARRS,* ***14W2****; C/2014 W2 Pan-STARRS,* ***41P****: 41P/Tuttle–Giacobini–Kresák,* ***14E2****: C/2014 E2 Jacques,* ***15V2****: C/2015 V2 Johnson.*

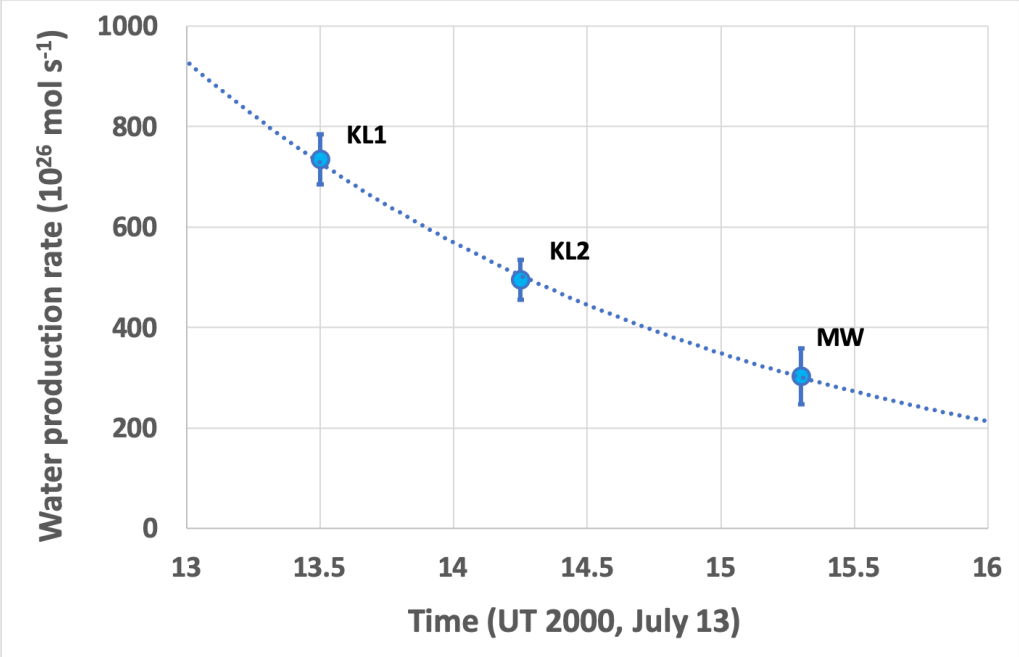

Figure 3. *Water production rate evolution in time for comet S4, during the 2000 observations. The blue dots are the retrieved water production rates reported with their uncertainties for each used setting (KL1, KL2, MW), while the dotted line represents an exponential fit to the data.*

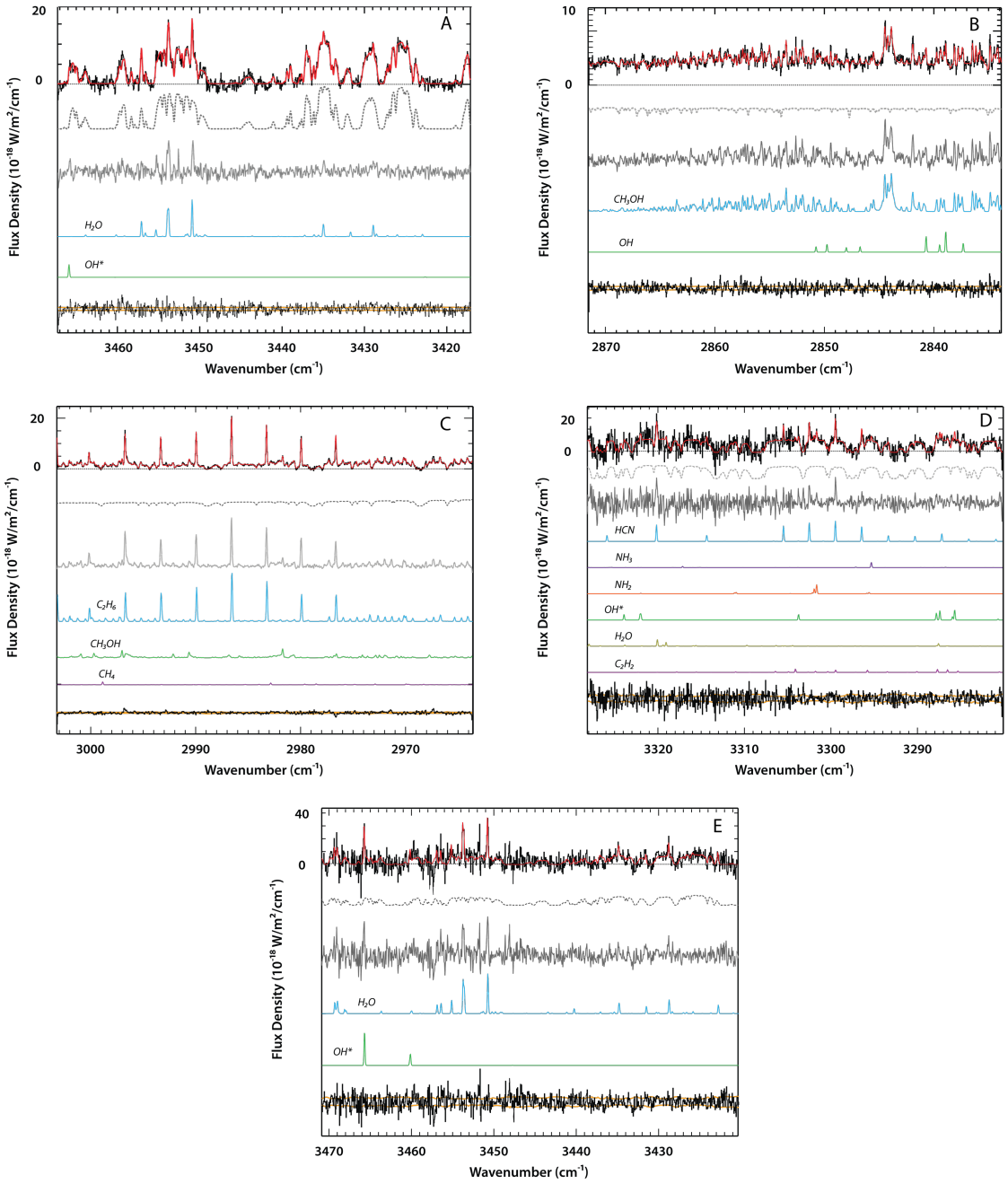

Figure 4. *Sample spectra for the re-analyzed comets. In each plot, the modeled spectrum, obtained using the Levenberg-Marquardt χ^2 algorithm, is plotted over the data in red; below the modeled spectrum, the dotted line represents the sum of atmospheric telluric and cometary continuum, while the grey line is the cometary spectrum after continuum subtraction; the quantum molecular models are represented by distinct colors below the spectra. The final black traces represent the residuals together with their corresponding ± 1σ errors (orange lines). Panel A – detection of H_2O and OH* in comet S4; Panel B – detection of CH_3OH and OH* in comet A2 (2001, July 9th); Panel C – detection of C_2H_6, CH_3OH and CH_4 in comet W1; Panel D – detection of HCN, NH_3, NH_2, OH*, H_2O and C_2H_2 in comet F6; Panel E – detection of H_2O and OH* in comet S1 (2012, November 7th).*

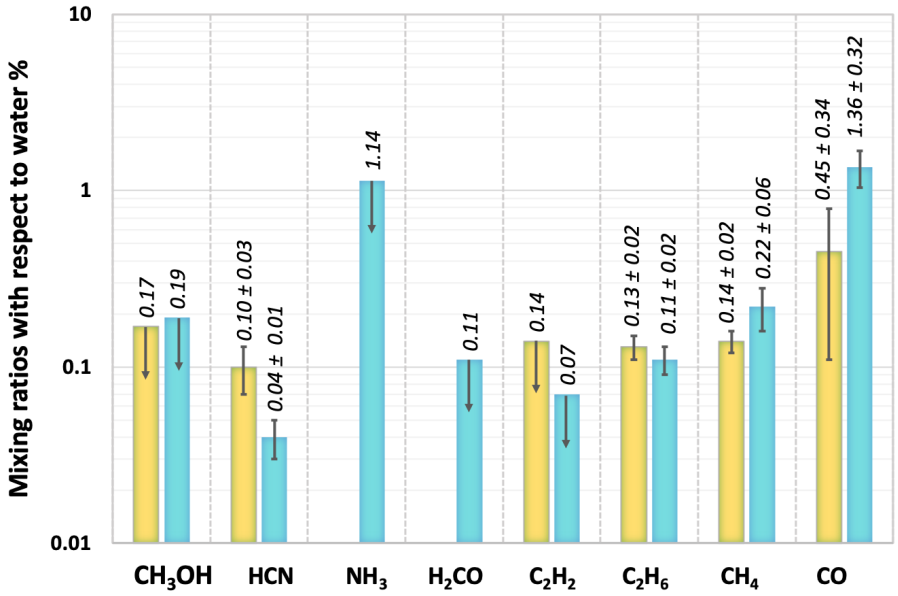

Figure 5. *Comparison of results presented in Mumma et al. 2001 (yellow bars) and this work (cyan bars), for comet S4. Mixing ratios for detected molecules are shown and reported together with the corresponding confidence limits, while 3σ upper limits are indicated with a downward arrow.*

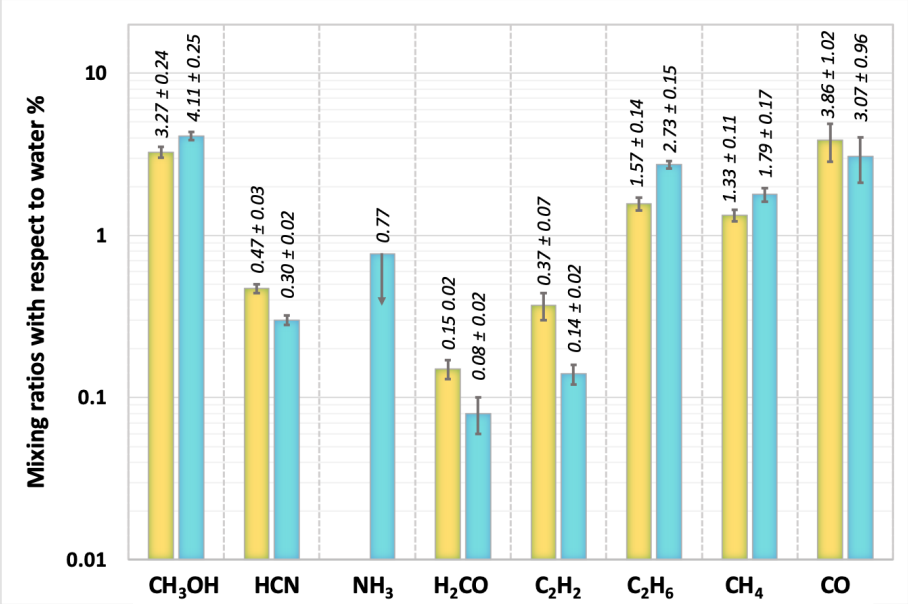

Figure 6*. Comparison of results presented in Magee Sauer et al. 2008 (yellow bars) and this work (cyan bars), for comet A2. Mixing ratios for detected molecules are shown and reported together with the corresponding confidence limits, while 3σ upper limits are indicated with a downward arrow.*

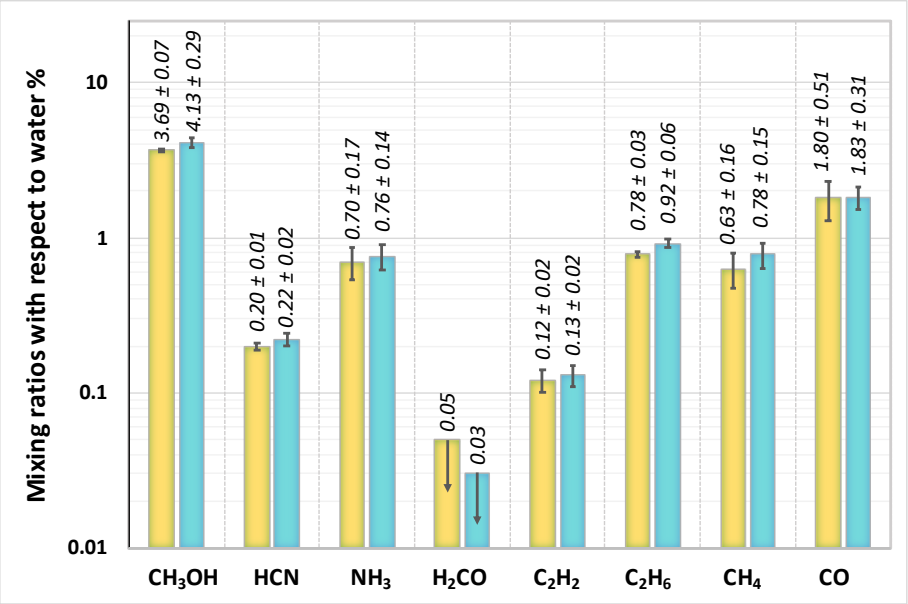

Figure 7. *Comparison of results presented in Villanueva et al. 2011a (yellow bars) and this work (cyan bars), for comet W1. Mixing ratios for detected molecules are shown and reported together with the corresponding confidence limits, while 3σ upper limits are indicated with a downward arrow.*

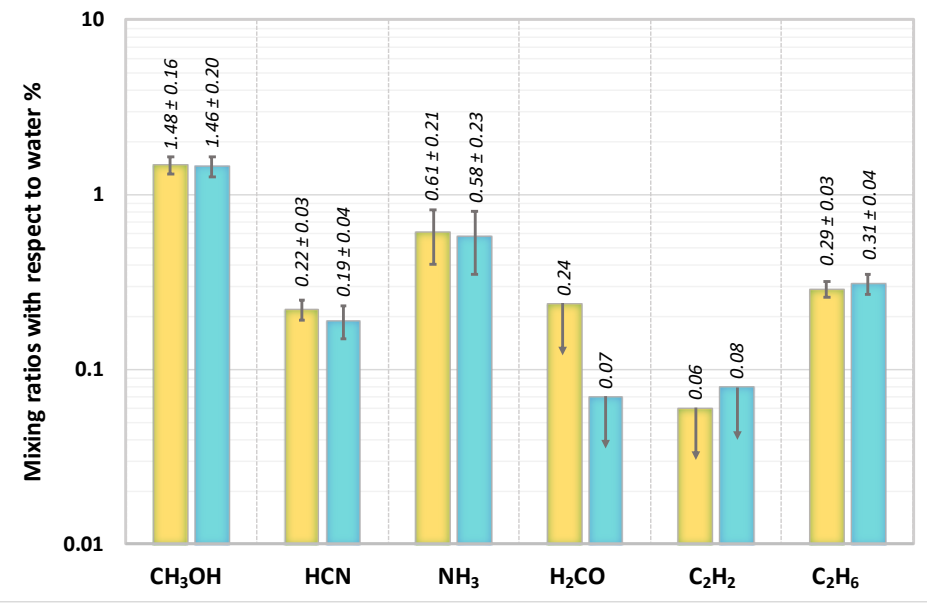

Figure 8. *Comparison of results presented in Paganini et al. 2014 (yellow bars) and this work (cyan bars), for comet F6. Mixing ratios for detected molecules are shown and reported together with the corresponding confidence limits, while 3σ upper limits are indicated with a downward arrow.*

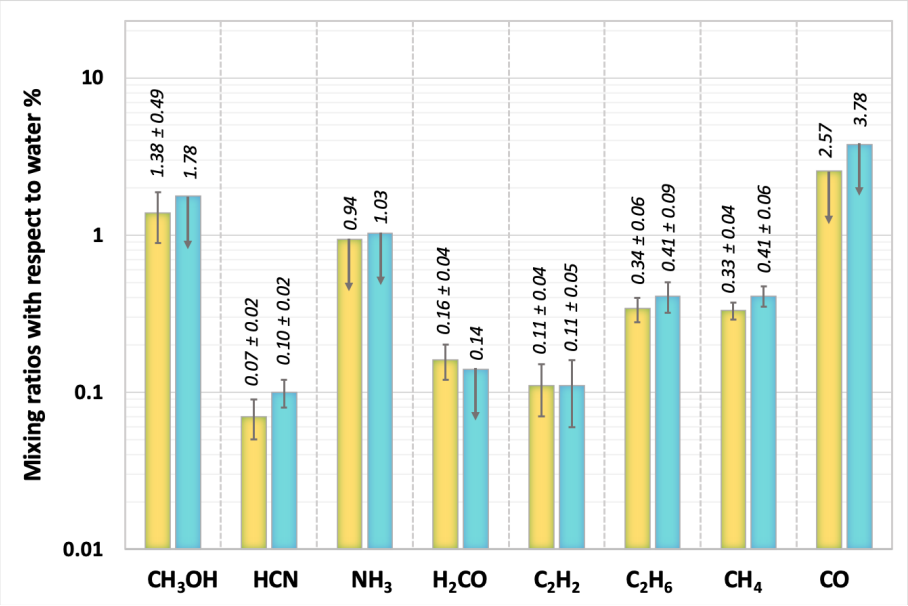

Figure 9. *Comparison of results presented in DiSanti et al. 2016 (yellow bars) and this work (cyan bars), for comet S1. Mixing ratios for detected molecules are shown and reported together with the corresponding confidence limits, while 3σ upper limits are indicated with a downward arrow.*

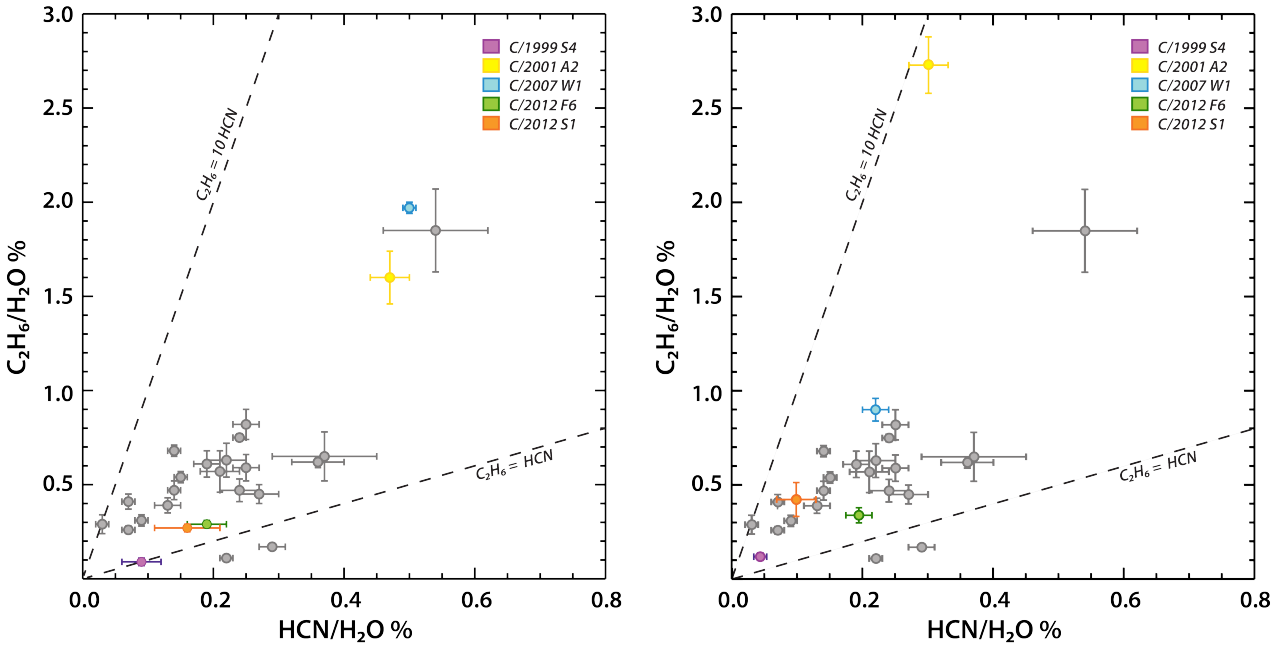

Figure 10. *Study of the correlation between HCN and C_2H_6 mixing ratios with respect to water before and after our revision of the data. The dark gray dots represent data for 21 comets (see Dello Russo et al. 2016 and references therein); the revised comets are indicated with different colors (S4 – violet, A2 – yellow, W1 – cyan, F6 – green, S1 – orange).*

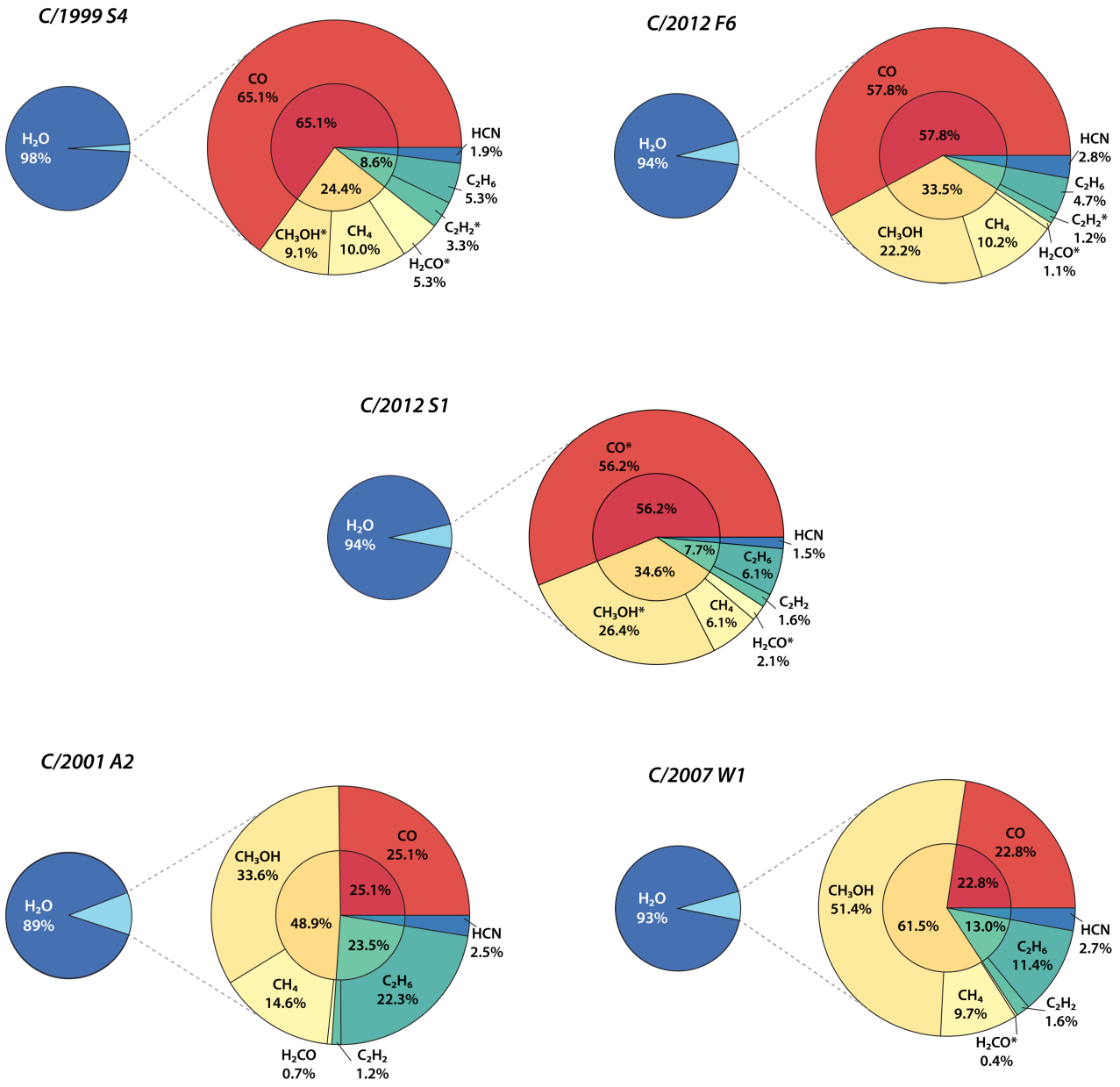

Figure 11. *Double level pie charts retrieved using the updated mixing ratios for the five analyzed comets, ordered with decreasing CO. Colors and groupings are described in the text. For every sector (i.e. molecule) the reported proportion is obtained normalizing the corresponding mixing ratio to the sum of all the considered mixing ratios obtained for that particular comet. Starred labels represent 3σ upper limits.*

Table 1: Observing logs for the analyzed comets

Date (UT)	*Setting*	*Principal molecules sampled*	R_h *(AU)*	V_h *(km s^{-1})*	*Δ (AU)*	V_Δ *(km s^{-1})*	*AM*	*Slit (arcsec)*
			C/1999 S4 (LINEAR)					
2000, Jul 13	KL1	H_2O, CH_3OH, C_2H_6	0.804	-10.33	0.547	-54.58	2.697	0.72
	KL2	H_2O, HCN, C_2H_2,NH_3, CH_4, H_2CO	0.804	-10.31	0.546	-54.51	2.281	0.72
	MW	H_2O, CO	0.804	-10.28	0.545	-54.38	1.810	0.72
			C/2001 A2 (LINEAR)					
2001, Jul 9	KL1	H_2O, CH_3OH, C_2H_6, CH_4	1.160	22.41	0.275	11.39	1.120	0.43
	KL2	H_2O, HCN, C_2H_2, NH_3, CH_4, H_2CO	1.161	22.42	0.276	11.57	1.020	0.43
2001, Jul 10	KL1	H_2O, CH_3OH, C_2H_6, CH_4	1.172	22.53	0.282	12.24	1.350	0.43
	KL2	H_2O, HCN, C_2H_2, NH_3, CH_4, H_2CO	1.173	22.54	0.282	12.40	1.110	0.43
	MW	H_2O, CO	1.175	22.55	0.283	12.83	1.061	0.43
			C/2007 W1 (Boattini)					
2008, Jul 9	KL1	H_2O, CH_3OH, C_2H_6, CH_4	0.893	9.77	0.348	12.91	1.910	0.43
	KL2	H_2O, HCN, C_2H_2, NH_3, CH_4, H_2CO	0.893	9.79	0.348	12.96	1.506	0.43
2008, Jul 10	MW	H_2O, CO	0.898	10.34	0.356	12.92	1.534	0.43
	KL2	H_2O, HCN, C_2H_2, NH_3, CH_4, H_2CO	0.899	10.36	0.356	12.98	1.899	0.43
			C/2012 F6 (Lemmon)					
2013, Jun 20	KL1	H_2O, CH_3OH, C_2H_6	1.737	24.29	1.790	5.26	1.787	0.43
	KL2	H_2O, HCN, C_2H_2, NH_3, CH_4, H_2CO	1.738	24.29	1.790	5.38	1.308	0.43
			C/2012 S1 (ISON)					
2013, Oct 22	MW	H_2O, CO	1.213	-38.05	1.502	-52.08	1.695	0.43
	KL1	H_2O, CH_3OH, C_2H_6	1.212	-38.06	1.502	-52.06	1.475	0.43
2013, Oct 24	MW	H_2O, CO	1.168	-38.75	1.443	-51.70	1.906	0.43
	KL1	H_2O, CH_3OH, C_2H_6	1.168	-38.77	1.442	-51.65	1.574	0.43
2013, Oct 25	KL2	H_2O, HCN, C_2H_2, NH_3, CH_4, H_2CO	1.146	-39.14	1.413	-51.41	1.620	0.43
2013, Nov 7	KL2	H_2O, HCN, C_2H_2, NH_3, CH_4, H_2CO	0.829	-45.91	1.056	-42.08	1.905	0.43

Notes: R_h is the heliocentric distance of the comet, V_h is the comet-sun relative velocity, Δ is the geocentric distance and V_Δ is the topocentric velocity; AM is the airmass. The values are given for the midpoint of the observing time interval.

Table 2: Production rates and mixing ratios with respect to water for comet S4

Molecule	*Setting*	*Total production rate [a] 10^{26} mol s^{-1}*	*Averaged mixing ratios %*
H_2O	KL1	735 ± 50	100
	KL2	495 ± 40	
	MW	303 ± 56	
CH_3OH	KL1	< 1.38	< 0.19
HCN	KL2	0.20 ± 0.08	0.04 ± 0.01
NH_3	KL2	< 5.64	< 1.14
H_2CO	KL2	< 0.56	< 0.11
C_2H_2	KL2	< 0.36	< 0.07
C_2H_6	KL1	0.81 ± 0.16	0.11 ± 0.02
CH_4	KL1	1.48 ± 0.55	0.22 ± 0.06
	KL2	1.17 ± 0.55	
CO	MW	4.11 ± 0.89	1.36 ± 0.32

Notes: All the production rates are calculated for a common rotational temperature of (75 ± 5)K.

a) Total production rate, after applying a measured growth factor (GF) of (1.47 ± 0.03) retrieved from water.

Table 3: Comparison of previous and updated rotational temperatures for comet S4

	Rotational temperatures (K)		
Molecule	*Mumma et al. 2001*	*Dello Russo et al. 2005*	*This work*
H_2O	(50)	$73\ ^{+8}_{-6}$	75 ± 5

Notes: values in parenthesis are assumed.

Table 4: Comparison of previous and updated water production rates for comet S4

	Water production rates 10^{26} mol s^{-1}		
Setting	*Mumma et al. 2001 [a]*	*Dello Russo et al. 2005 [b]*	*This work*
KL1	730 ± 50 (OH*)	673 ± 56	735 ± 50
KL2	730 ± 50 (OH*)	673 ± 119	495 ± 40
MW	446 ± 72		303 ± 56

a) Mumma et. al 2001 retrieved a water production rate of (446 ± 72) x 10^{26} mol s^{-1} using two H_2O lines in the MW setting. For the KL1 and KL2 settings their reported production rate of (730 ± 50) x 10^{26} mol s^{-1} was computed from spectral lines of OH (prompt emission). They used the weighted mean of the MW and KL values ((638 ± 44) x 10^{26} mol s^{-1})) when computing mixing ratios for UT 13 July 2000; b) Dello Russo et al. 2005 introduced a new model for H_2O lines detected in KL1 and KL2.*

Table 5: Comparisons of previous and current mixing ratios for comet S4

Molecule	*Previous results*	*This work*	*Relative difference %*
CH_3OH	< 0.17 [a] < 0.15 [b]	< 0.19	12% 27%
HCN	0.10 ± 0.03 [a] 0.08 ± 0.02 [b]	0.04 ± 0.01	-60% -56%
NH_3		< 1.14	
H_2CO		< 0.11	
C_2H_2	< 0.14 [a] < 0.12 [b]	< 0.07	-50% -46%
C_2H_6	0.13 ± 0.02 [a] 0.11 ± 0.02 [b]	0.11 ± 0.02	-15% -8%
CH_4	0.15 ± 0.02 [a] 0.14 ± 0.02 [b] 0.18 ± 0.06 [c]	0.22 ± 0.06	57% 47% 22%
CO	0.45 ± 0.34 [a] 0.28 ± 0.21 [b]	1.36 ± 0.32	202% 354%

a) Mumma et al. 2001; b) Dello Russo et al. 2005; c) Gibb et al. 2003.

Table 6: Comparison of rotational temperatures for comet A2

		Rotational temperatures (K)	
Molecule	***Date (2001 UT)***	***Magee Sauer et al. 2008***	***This work***
H_2O	Jul 9	98^{+6}_{-5}	88 ± 6
	Jul 10	105^{+5}_{-3}	78 ± 9
C_2H_6	Jul 9	102^{+13}_{-12}	86 ± 5
	Jul 10		82 ± 4
CH_3OH [a]	Jul 9		82^{+5}_{-6}
	Jul 10		79 ± 4
HCN	Jul 9	56 ± 6	66^{+7}_{-8}
	Jul 10	67 ± 4	67^{+5}_{-4}
CO	Jul 10	126^{+42}_{-36}	
H_2CO	Jul 9	104^{+20}_{-18}	

a) Villanueva et al. 2012a retrieved a rotational temperature of (78 ± 5) K on UT 9.5 July for CH_3OH, using the updated molecular model, in agreement with current results.

Table 7: Production rates and mixing ratios with respect to water for comet A2

Date (UT 2001)	***Molecule***	***Total production rates [a] 10^{26} mol s^{-1}***	***Averaged mixing ratios % [b]***
Jul 9	H_2O [c]	284 ± 29	100
Jul 10		278 ± 18	
Jul 10	H_2O [d]	293 ± 77	
Jul 9	CH_3OH	14.5 ± 0.6	4.11 ± 0.25
Jul 10		10.6 ± 0.5	
Jul 9	HCN[e]	0.86 ± 0.09	0.30 ± 0.02
Jul 10		0.84 ± 0.05	
Jul 9	NH_3	< 2.60	< 0.77
Jul 10		< 2.13	
Jul 9	H_2CO	0.23 ± 0.08	0.08 ± 0.02
Jul 10		< 0.17	
Jul 9	C_2H_2	0.41 ± 0.11	0.14 ± 0.02
Jul 10		0.38 ± 0.06	
Jul 9	C_2H_6	9.11 ± 0.24	2.73 ± 0.15
Jul 10		7.16 ± 0.25	
Jul 9	CH_4	4.74 ± 0.75	1.79 ± 0.17
Jul 10		5.10 ± 0.44	
Jul 10	CO	9.0 ± 2.0	3.07 ± 0.96

Notes: All the production rates are calculated for a common rotational temperature of (85 ± 5)K.
a) Global production rates, after applying the following measured growth factors: 9 July – (1.60 ± 0.03) (retrieved from H_2O, CH_3OH, C_2H_6 and HCN), 10 July - (1.50 ± 0.03) (retrieved from H_2O, CH_3OH, C_2H_6 and HCN); b) the averaged mixing ratio is calculated as the weighted average of the singular mixing ratios obtained for the different observing nights; c) obtained combining KL1 and KL2 settings; d) MW setting; e) the HCN mixing ratio for a temperature of (67 ± 4) is about (0.29 ± 0.03), that is comparable within 1σ with the one extracted for T_{rot} = (85 ± 5).

Table 8: Comparison of water production rates for comet A2

		Water production rates 10^{26} mol s^{-1}	
Date (2001 UT)	***Settings***	***Magee Sauer et al. 2008***	***This work***
Jul 9	KL1 + KL2	377 ± 34	284 ± 29
Jul 10	KL1 + KL2	430 ± 37	278 ± 18
Jul 10	MW	424 ± 40	293 ± 77

Table 9: Relative differences between previous and current mixing ratios for comet A2

Molecule	*Previous results [a]*	*This work*	*Relative difference %*
CH_3OH	3.27 ± 0.24 2.99 ± 0.11 [b]	4.11 ± 0.25	25% 37%
HCN	0.47 ± 0.03	0.30 ± 0.02	-36%
NH_3		< 0.77	
H_2CO	0.15 ± 0.02	0.08 ± 0.02	-47%
C_2H_2	0.37 ± 0.07	0.14 ± 0.02	-62%
C_2H_6	1.57 ± 0.14	2.73 ± 0.15	74%
CH_4	1.33 ± 0.11	1.79 ± 0.17	35%
CO	3.86 ± 1.02	3.07 ± 0.96	-20%

a) All previous values are taken from Magee Sauer et al. 2008 and references therein, considering only production rates on the 9th and 10th of July 2001; b) after Villanueva et al. 2012a, based on the previous water production rate of Magee-Sauer et al 2008.

Table 10: Production rates and mixing ratios with respect to water for comet W1

Date (UT 2008)	*Molecule*	*Production rates [a] 10^{26} mol s^{-1}*	*Averaged mixing ratios % [b]*
9 Jul	H_2O [c]	272 ± 15	100
10 Jul	H_2O [d]	264 ± 20	
9 Jul	CH_3OH	11.7 ± 0.9	4.13 ± 0.29
10 Jul		10.4 ± 0.8	
9 Jul	HCN	0.61 ± 0.04	0.22 ± 0.02
9 Jul	NH_3	2.07 ± 0.36	0.76 ± 0.14
9 Jul	H_2CO	< 0.08	< 0.03
9 Jul	C_2H_2	0.34 ± 0.04	0.13 ± 0.02
9 Jul	C_2H_6	2.59 ± 0.17	0.92 ± 0.06
10 Jul		2.35 ± 0.15	
9 Jul	CH_4 [c]	2.13 ± 0.38	0.78 ± 0.15
10 Jul	CO	4.84 ± 0.72	1.83 ± 0.31

Notes: All production rates are calculated for an average rotational temperature of (83 ± 4) K.
a) Global production rates after applying measured growth factors of (1.39 ± 0.10) to H_2O and CH_3OH, and (1.63 ± 0.10) to other trace species, and a correction factor of 2.5 to H_2O and CH_3OH (see Villanueva et al. 2011 for a more detailed explanation); b) weighted average of the mixing ratios obtained for the different observing nights; c) obtained combining KL1 and KL2 settings; d) obtained combining KL1 and MW settings.

Table 11: Comparison of previous and updated rotational temperatures for comet W1

Rotational temperatures (K)			
Molecule	**Date (2008 UT)**	**Villanueva et al. 2011a**	**This work**
H_2O	Jul 9	80 ± 2	83 ± 4
	Jul 10	79 ± 3	83 ± 3
C_2H_6	Jul 9	79 ± 3	80 ± 3
	Jul 10	78 ± 3	78^{+5}_{-4}
HCN	Jul 9	84 ± 5	84^{+7}_{-6}
CH_3OH	Jul 9		83^{+5}_{-4}
	Jul 10		83^{+5}_{-4}

Table 12: Comparison of previous and updated water production rates for comet W1

Water production rates 10^{26} mol s^{-1}			
Date (UT)	**Settings**	**Villanueva et al. 2011a**	**This work**
Jul 9	KL1 + KL2	301 ± 22	272 ± 15
Jul 10	KL1 + MW	306 ± 23	264 ± 20

Table 13: Relative differences between previous and updated mixing ratios for comet W1.

Molecule	**Villanueva et al. 2011a**	**This work**	**Relative difference%**
CH_3OH	3.69 ± 0.07	4.13 ± 0.29	12%
HCN	0.20 ± 0.01	0.22 ± 0.02	10%
NH_3	0.70 ± 0.17	0.76 ± 0.14	9%
H_2CO	< 0.05	< 0.03	-0.4%
C_2H_2	0.12 ± 0.02	0.13 ± 0.02	8%
C_2H_6	0.78 ± 0.03	0.92 ± 0.06	18%
CH_4	0.63 ± 0.16	0.78 ± 0.15	24%
CO	1.80 ± 0.51	1.83 ± 0.31	2%

Table 14: Production rates and mixing ratios with respect to water for comet F6

Molecule	*Production rates [a] 10^{26} mol s^{-1}*	*Averaged mixing ratios %*
H_2O [b]	1160 ± 97	100
CH_3OH	16.9 ± 1.8	1.46 ± 0.20
HCN	2.24 ± 0.36	0.19 ± 0.04
NH_3	6.69 ± 2.63	0.58 ± 0.23
H_2CO	< 0.78	< 0.07
C_2H_2	< 0.93	< 0.08
C_2H_6	3.63 ± 0.36	0.31 ± 0.04

Notes: All the production rates are calculated for an average temperature of (53 ± 3)K.
a) Global production rates after applying measured growth factors of (2.63 ± 0.14) to H_2O and (1.63 ± 0.06) to other trace species; b) combination of KL1 and KL2 settings

Table 15: Comparison of previous and updated rotational temperatures for comet F6

Rotational temperatures (K)		
Molecule	*Paganini et al. 2014*	*This work*
H_2O	50^{+7}_{-6}	53 ± 3
C_2H_6	59^{+14}_{-10}	50 ± 3
CH_3OH	50^{+7}_{-5}	45^{+11}_{-8}
HCN		41^{+10}_{-7}

Table 16: Comparison of previous and updated water production rates for comet F6

Water production rates 10^{26} mol s^{-1}		
Settings	*Paganini et al. 2014*	*This work*
KL1 + KL2	1054 ± 66	1160 ± 97

Table 17: Relative differences between previous and updated mixing ratios for comet F6

Molecule	*Paganini et al. 2014*	*This work*	*Relative difference%*
CH_3OH	1.48 ± 0.16	1.46 ± 0.20	-1%
HCN	0.22 ± 0.03	0.19 ± 0.04	-14%
NH_3	0.61 ± 0.21	0.58 ± 0.23	-5%
H_2CO	< 0.24	< 0.07	-71%
C_2H_2	< 0.06	< 0.08	33%
C_2H_6	0.29 ± 0.03	0.31 ± 0.04	7%

Table 18: Production rates and mixing ratios with respect to water for comet S1

Date (UT 2012)	**Molecule**	**Production rates [a] 10^{26} mol s^{-1}**	**Averaged mixing ratios % [b]**
Oct 22	H_2O	116 ± 15	100
Oct 24		85 ± 8 [c]	
Oct 25		71 ± 19	
Nov 7		395 ± 34	
Oct 22	CH_3OH	< 2.06	< 1.78
Oct 24		< 2.80	
Oct 25	HCN	< 0.15	0.10 ± 0.02
Nov 7		0.38 ± 0.11	
Oct 25	NH_3	< 2.07	< 1.03
Nov 7		< 4.05	
Oct 25	H_2CO	< 0.25	< 0.14
Nov 7		< 0.54	
Oct 25	C_2H_2	< 0.28	0.11 ± 0.05
Nov 7		0.43 ± 0.19	
Oct 22	C_2H_6	0.45 ± 0.14	0.41 ± 0.09
Oct 24		0.37 ± 0.12	
Oct 25	CH_4	0.19 ± 0.12	0.41 ± 0.06
Nov 7		1.85 ± 0.35	
Oct 24	CO	< 3.21	< 3.78

Notes: production rates are calculated using an average temperature of 50 K (assumed) for the first two nights, (53 ± 5) K for the third night and (63 ± 4) K for the last night
a) Global production rates after applying measured growth factors of (1.72 ± 0.12) for the 22nd of October, (1.61 ± 0.10) for the 24th of October, (1.42 ± 0.22) for the 25th of October and (1.98 ± 0.30) for the 7th of November; b) mixing ratios are calculated as the weighted average of the singular mixing ratios obtained for the different observing nights; c) obtained from the combination of KL1 and MW settings.

Table 19: Comparison of previous and updated rotational temperatures for comet S1

Rotational temperatures (K)			
Molecule	***Date (2013 UT)***	***DiSanti et al. 2016***	***This work***
H_2O	Oct 22	52 ± 19	(50)
	Oct 24	(50)	(50)
	Oct 25	(50)	53 ± 5
	Nov 7	(70)	63 ± 4

Table 20: Comparison of previous and updated water production rates for comet S1

Water production rates 10^{26} mol s^{-1}			
Date (2013 UT)	***Settings***	***DiSanti et al. 2016***	***This work***
Oct 22	KL1	110 ± 14	116 ± 15
Oct 24	KL1 + MW	92.4 ± 8.4	85 ± 8
Oct 25	KL2	63 ± 15	71 ± 19
Nov 7	KL2	400 ± 71	395 ± 34

Table 21: Relative differences between previous and updated mixing ratios for comet S1

Molecule	***DiSanti et al. 2016***	***This work***	***Relative difference%***
CH_3OH	1.38 ± 0.49	< 1.78	29%
HCN	0.074 ± 0.016	0.10 ± 0.02	43%
NH_3	< 0.94	< 1.03	10%
H_2CO	0.16 ± 0.04	< 0.14	-13%
C_2H_2	0.11 ± 0.04	0.11 ± 0.05	0%
C_2H_6	0.34 ± 0.06	0.41 ± 0.09	21%
CH_4	0.33 ± 0.04	0.41 ± 0.06	24%
CO	< 2.57	< 3.78	47%

Acknowledgments

This work was supported by the NASA Astrobiology Institute (13-13NAI7-0032 to Goddard Space Flight Center, PI M. J. Mumma) and the NASA Emerging Worlds Program (EW15-57 to Goddard Space Flight Center, PI G. L. Villanueva). This research has made use of the Keck Observatory Archive (KOA), which is operated by the W. M. Keck Observatory and the NASA Exoplanet Science Institute (NExScI), under contract with the National Aeronautics and Space Administration.

The authors wish to recognize and acknowledge the very significant cultural role and reverence that the summit of Mauna Kea has always had within the indigenous Hawaiian community. We are most fortunate to have the opportunity to conduct observations from this mountain.

Bibliography

Bockelée-Morvan D. and Biver N., 2017. The composition of cometary ices. Philosophical Transactions of the Royal Society A: Mathematical, Physical and Engineering Sciences, 375, 20160252. http://doi.org/10.1098/rsta.2016.0252.

Bockelée -Morvan, D., Biver, N., Moreno, R., Colom, P., Crovisier, J., Gerard, E., Henry, F., Lis, D.C., Matthews, H., Weaver, H.A., Womack, M., Festou, M.C., 2001. Outgassing Behavior and Composition of Comet C/1999 S4 (LINEAR) During Its Disruption. Science 292, 1339–1343. doi:10.1126/science. 1058512.

Bockelée -Morvan, D., Crovisier, J., 1989. The nature of the 2.8-micron emission feature in cometary spectra. Astronomy and Astrophysics 216, 278–283.

Bockelée -Morvan, D., Brooke, T.Y., Crovisier, J., 1995. On the origin of the 3.2 to 3.6-micron emission features in comets. Icarus 116, 18–39. doi:10.1006/icar.1995.1111.

Bonev, B.P., 2005. Towards a Chemical Taxonomy of Comets: Infrared Spectroscopic Methods for Quantitative Measurements of Cometary Water. Ph.D. thesis. The University of Toledo.

Bonev, B.P., Mumma, M.J., DiSanti, M.A., Dello Russo, N., Magee-Sauer, K., Ellis, R.S., Stark, D.P., 2006. A Comprehensive Study of Infrared OH Prompt Emission in Two Comets. I. Observations and Effective g-Factors. Astrophysical Journal 653, 774–787. doi:10.1086/508452.

Bonev, B.P., Villanueva, G.L., Paganini, L., DiSanti, M.A., Gibb, E.L., Keane, J.V., Meech, K.J., Mumma, M.J., 2013. Evidence for two modes of water release in Comet 103P/Hartley 2: Distributions of column density, rotational temperature, and ortho-para ratio. Icarus 222, 740–751. doi:10.1016/j.icarus.2012.07.034.

Clough, S.A., Shephard, M.W., Mlawer, E.J., Delamere, J.S., Iacono, M.J., Cady-Pereira, K., Boukabara, S., Brown, P.D., 2005. Atmospheric radiative transfer modeling: a summary of the AER codes. Journal of Quantitative Spectroscopy and Radiative Transfer 91, 233–244. doi:10.1016/j.jqsrt.2004.05.058.

Dello Russo, N., Bonev, B.P., DiSanti, M.A., Mumma, M.J., Gibb, E.L., Magee-Sauer, K., Barber, R.J., Tennyson, J., 2005a. Water Production Rates, Rotational Temperatures, and Spin Temperatures in Comets C/1999 H1 (Lee), C/1999 S4, and C/2001 A2. Astrophysical Journal 621, 537–544. doi:10. 1086/427473.

Dello Russo, N., DiSanti, M.A., Mumma, M.J., Magee-Sauer, K., Rettig, T.W., 1998. Carbonyl Sulfide in Comets C/1996 B2 (Hyakutake) and C/1995 O1 (Hale-Bopp): Evidence for an Extended Source in Hale-Bopp. Icarus 135, 377–388. doi:10.1006/icar.1998.5990.

Dello Russo, N., Kawakita, H., Vervack, R.J., Weaver, H.A., 2016. Emerging trends and a comet taxonomy based on the volatile chemistry measured in thirty comets with high-resolution infrared spectroscopy between 1997 and 2013. Icarus 278, 301–332. doi:10.1016/j.icarus.2016.05.039.

Dello Russo, N., Mumma, M.J., DiSanti, M.A., Magee-Sauer, K., Novak, R., 2001. Ethane Production and Release in Comet C/1995 O1 Hale-Bopp. Icarus 153, 162-179. doi:10.1006/icar.2001.6678.

DiSanti, M.A., Bonev, B.P., Gibb, E.L., Paganini, L., Villanueva, G.L., Mumma, M.J., Keane, J.V., Blake, G.A., Dello Russo, N., Meech, K.J., Vervack, R. J., J., McKay, A.J., 2016. Enroute to Destruction: The Evolution in Composition of Ices in Comet D/2012 S1 (ISON) between 1.2 and 0.34 AU from the Sun as Revealed at Infrared Wavelengths. Astrophysical Journal 820, 34. doi:10.3847/ 0004-637X/820/1/34.

DiSanti, M.A., Bonev, B.P., Magee-Sauer, K., Dello Russo, N., Mumma, M.J., Reuter, D.C., Villanueva, G.L., 2006. Detection of Formaldehyde Emission in Comet C/2002 T7 (LINEAR) at Infrared Wavelengths: Line-by-Line Validation of Modeled Fluorescent Intensities. Ap. J. 650, 470.

Edwards, D.P., 1992, GENLN2: A general line-by-line atmospheric transmittance and radiance model. Version 3.0: Description and users guide.

Farnham, T.L., Schleicher, D.G., Woodney, L.M., Birch, P.V., Eberhardy, C.A., Levy, L., 2001. Imaging and Photometry of Comet C/1999 S4 (LINEAR) Before Perihelion and After Breakup. Science 292, 1348–1354. doi:10.1126/science.1058886.

Gelaro, R., McCarty, W., Suarez, M.J., Todling, R., Molod, A., Takacs, L., et al. The modern-era retrospective analysis for research and applications, version 2 (MERRA-2). J. Clim. 2017;30:5419–54. doi: 10.1175/JCLI- D- 16- 0758.1 .

Gibb, E. L., Bonev, B. P., Villanueva, G. L., DiSanti, M. A., Mumma, M. J. 2013. Solar fluorescence model of CH_3D as applied to comet emission. J. Mol. Spec. 291, 118.

Gibb, E.L., DiSanti, M.A., Magee-Sauer, K., Dello Russo, N., Bonev, B.P., Mumma, M.J., 2007. The organic composition of C/2001 A2 (LINEAR). II. Search for heterogeneity within a comet nucleus. Icarus 188, 224–232. doi:10.1016/j.icarus.2006.11.009.

Gibb, E.L., Mumma, M.J., Dello Russo, N., DiSanti, M.A., Magee-Sauer, K., 2003. Methane in Oort cloud comets. Icarus 165, 391–406. doi:10.1016/S0019-1035(03)00201-X.

Gomes, R.; Levison, H. F.; Tsiganis, K.; Morbidelli, A., 2005. Origin of the cataclysmic Late Heavy Bombardment period of the terrestrial planets. Nature 435, 466–469.

Hiraoka, K., Ohashi, N., Kihara, Y., Yamamoto, K., Sato, T., Yamashita, A. 1994. Formation of formaldehyde and methanol from the reactions of H atoms with solid CO at 10-20 K. Chemical Physics Letters 229, 408-414.

Hiraoka, K., Miyagoshi, T., Takayama, T., Yamamoto, T., & Kihara, Y., 1998. Gas-grain processes for the formation of CH_4 and H_2O: Reactions of H atoms with C, O, and CO in the solid phase at 12K. Astrophysical Journal 498, 710-715. doi: 10.1086/305572.

Hiraoka, K., Takayama, T., Euchi, A., Handa, H., and Sato, T. 2000. Study of the reactions of H and D atoms with soid C_2H_2, C_2H_4, and C_2H_6 at cryogenic temperatures. Astrophysical Journal 532. 1029-1037. doi: 10.1086/308612

Hoban, S., Mumma, M., Reuter, D.C., DiSanti, M., Joyce, R.R., Storrs, A., 1991. A Tentative Identification of Methanol as the Progenitor of the 3.52-µm Emission Feature in Several Comets. Icarus 93, 122–134. doi:10.1016/0019-1035(91)90168-S.

Kunde, V.R., Maguire, W.C., 1974. Direct integration transmittance model. Journal of Quantitative Spectroscopy and Radiative Transfer 14, 803–817. doi:10.1016/0022-4073(74)90124-1.

Magee-Sauer, K., Mumma, M.J., DiSanti, M.A., Dello Russo, N., Gibb, E.L., Bonev, B.P., Villanueva, G.L., 2008. The organic composition of Comet C/2001 A2 (LINEAR). I. Evidence for an unusual organic chemistry. Icarus 194, 347–356. doi:10.1016/j.icarus.2007.10.006.

Magee-Sauer, K., Mumma, M.J., DiSanti, M.A., Dello Russo, N., 2002. Hydrogen cyanide in comet C/1996 B2 Hyakutake. Journal of Geophysical Research (Planets) 107, 5096. doi:10.1029/ 2002JE001863.

McLean, I., E. Becklin, E., Bendiksen, O., Brims, G., Canfield, J., F. Figer, D., R. Graham, J., Hare, J., Lacayanga, F., E. Larkin, J., B. Larson, S., G. Levenson, N., Magnone, N., I. Teplitz, H., Wong, W., 1998. Design and development of NIRSPEC: a near-infrared echelle spectrograph for the Keck II telescope. Proceedings of SPIE - The International Society for Optical Engineering 3354, 566–578. doi:10.1117/12.317283.

Morbidelli, A., Tsiganis, A., Krida, A., Levison, H. F., Gomes. R., 2007. Dynamics of the Giant Planets of the Solar System in the Gaseous Proto- planetary Disk and Their Relationship to the Current Orbital Architecture. Astronomical Journal 134, 1790–1798. doi:10.1086/521705

Mumma, M.J., DiSanti, M.A., Tokunaga, A.T., Roettger, E.E., 1995. Ground-based Detection of Water in Comets Shoemaker-Levy 1992 XIX and 6P/d'Arrest: Probing Parent Volatiles by hot-band Fluorescence. Bull. Amer. Astron. Soc. 27, No. 3: 1144.

Mumma, M.J., Dello Russo, N., DiSanti, M.A., Magee-Sauer, K., Novak, R.E., Brittain, S., Rettig, T., McLean, I.S., Reuter, D.C., Xu, L.H., 2001. Organic Composition of C/1999 S4 (LINEAR): A Comet Formed Near Jupiter? Science 292, 1334–1339. doi:10.1126/science.1058929.

Mumma, M.J., DiSanti, M.A., Dello Russo, N., Fomenkova, M., Magee-Sauer, K., Kaminski, C.D., Xie, D.X., 1996. Detection of Abundant Ethane and Methane, along with Carbon Monoxide and Water, in Comet C/1996 B2 Hyakutake: Evidence for Interstellar Origin. Science 272, 1310–1314. doi:10.1126/ science.272.5266.1310.

Mumma, M.J., DiSanti, M.A., Dello Russo, N., Magee-Sauer, K., Gibb, E., Novak, R., 2003. Remote infrared observations of parent volatiles in comets: A window on the early solar system. Advances in Space Research 31, 2563–2575. doi:10.1016/S0273-1177(03)00578-7.

Mumma, M. J. and Charnley, S. B., 2011. The Chemical Composition of Comets — Emerging Taxonomies and Natal Heritage. Ann. Rev. of Astron. and Astrophys 49, 471-524. Doi: 10.1146/annurev-astro-081309-130811

Paganini, L., DiSanti, M.A., Mumma, M.J., Villanueva, G.L., Bonev, B.P., Keane, J.V., Gibb, E.L., Boehnhardt, H., Meech, K.J., 2014. The Unexpectedly Bright Comet C/2012 F6 (Lemmon) Unveiled at Near-infrared Wavelengths. Astronomical Journal 147, 15. doi:10.1088/0004-6256/147/1/15.

Reuter, D.C., 1992. The Contribution of Methanol to the 3.4 Micron Emission Feature in Comets. Astrophysical Journal 386, 330. doi:10.1086/171019.

Rothman, L.S., Gamache, R.R., Tipping, R.H., Rinsland, C.P., Smith, M.A.H., Benner, D.C., Devi, V.M., Flaud, J.M., Camy-Peyret, C., Perrin, A., 1992. The HITRAN molecular data base - Editions of 1991 and 1992. Journal of Quantitative Spectroscopy and Radiative Transfer 48, 469–507. doi:10. 1016/0022-4073(92)90115-K.

Villanueva, G.L., DiSanti, M.A., Mumma, M.J., Xu, L.H., 2012a. A quantum band model of the ν_3 fundamental of methanol (CH_3OH) and its applications to fluorescence spectra of comets. Astrophysical Journal 747, 37. doi:10.1088/0004-637x/747/1/37.

Villanueva, G.L., Mumma, M.J., Bonev, B.P., Novak, R.E., Barber, R.J., DiSanti, M.A., 2012b. Water in planetary and cometary atmospheres: H_2O/HDO transmittance and fluorescence models. Journal of Quantitative Spectroscopy and Radiative Transfer 113, 202–220. doi:10.1016/j.jqsrt.2011.11.001.

Villanueva, G.L., Mumma, M.J., DiSanti, M.A., Bonev, B.P., Gibb, E.L., Magee-Sauer, K., Blake, G.A., Salyk, C., 2011a. The molecular composition of Comet C/2007 W1 (Boattini): Evidence of a peculiar outgassing and a rich chemistry. Icarus 216, 227–240. doi:10.1016/j.icarus.2011.08.024.

Villanueva, G.L., Mumma, M.J., Magee-Sauer, K., 2011b. Ethane in planetary and cometary atmospheres: Transmittance and fluorescence models of the ν_7 band at 3.3 μm. Journal of Geophysical Research (Planets) 116, E08012. doi:10.1029/2010JE003794.

Villanueva, G.L., Mumma, M.J., Novak, R.E., Hewagama, T., 2008. Identification of a new band system of isotopic CO_2 near 3.3 μm: Implications for remote sensing of biomarker gases on Mars. Icarus 195, 34–44. doi:10.1016/j.icarus.2007.11.014.

Villanueva, G.L., Smith, M.D., Protopapa, S., Faggi, S., Mandell, A.M., 2018. Planetary Spectrum Generator: An accurate online radiative transfer suite for atmospheres, comets, small bodies and exoplanets. Journal of Quantitative Spectroscopy and Radiative Transfer 217, 86–104. doi:10.1016/ j.jqsrt.2018.05.023, arXiv:1803.02008.

Villanueva, G.L., Mumma, M.J., Novak, R.E., Radeva, Y.L., Käufl , H.U., Smette, A., Tokunaga, A., Brown, P. D., Khayat, A., Encrenaz, T., Hartog, P., 2012. A sensitive search for organics (CH_4, CH_3OH, H_2CO, C_2H_6, C_2H_2, C_2H_4), hydroperoxyl (HO_2), nitrogen compounds (N_2O, NH_3, HCN) and chlorine species (HCL, CH_3CL) on Mars using ground-based high-resolution infrared spectroscopy. Icarus 223, 11 – 27, doi:https://doi.org/10.1016/j.icarus.2012.11.013

Weaver, H.A., Mumma, M.J., Larson, H.P., Davis, D.S., 1986. Post-perihelion observations of water in comet Halley. Nature 324, 441–444. doi:10.1038/324441a0.